

## Analysis the thermal properties of blocks made from ashes of natural fibers and construction waste

by F. C. Silveira\*, J. C. Cardoso\*, S. P. M. Franco\*, M. C. de Barros Jr\*, S. G. Tavares\*

\*Instituto de Engenharia e Tecnologia, Centro Universitário de Belo Horizonte – UNIBH, Av. Professor Mário Werneck, 1685, CEP 30455-610, Belo Horizonte, Brazil, [sinthyta.tavares@unibh.br](mailto:sinthyta.tavares@unibh.br)

### Abstract

In this work the infrared thermography is applied to the determinate thermal properties of blocks made from construction waste and natural fibbers. To perform the analysis were used three types of blocks where part of the cement was replaced by rice husk ashes and coffee husk ashes. Analysis was used for pulsed thermography. A mathematical model was implemented in order to validate the results obtained experimentally by thermographic technique. The results are always been presented correlated with the evaluated measurement uncertainty.

### 1. Introduction

The construction industry is one of the industries that more produce impacts on natural resources. It changes the environment from the installation of the work, cleaning up the same [1]. The large amount of waste generated by this industry, in most cases is disposed of illegally in big cities, worsening urban problems [2].

In order to reduce costs by removing the debris and also use it in some way, the city of Belo Horizonte created a group called Ecobloco, where they receive the rubble transforming them in building blocks for use in building civil. The waste that can be used for the manufacture of the blocks are: mortars, concrete, conventional natural aggregates, cement, bricks, ceramic plates and blocks. These correspond to approximately 80% of waste generated. The use of waste in the manufacture of blocks is also a way to reduce cost without reducing quality. Thus, in order to improve the tensile strength and compression of these blocks, studies were made for the inclusion of vegetable fibers in them, in form of raw or ashes. Studies done with the ashes of vegetable fibers intended to replace the cement in the production of the block, while maintaining and even improving quality. The cement is one of more materials consumed in the entire world, even surpassing the water intake (considering the loss after treatment), therefore, the use of alternative materials to match the compound is required [3].

Many of the food processing industries also generate waste. Without a final destination they end up being dumped on the roadsides and rivers. The rice processing industries, for example, are the main consumers of the shell of the grain, using them as a source fuel, but the ash generated has no commercial value. The companies, being small, does not have the same methods for reuse or disposal of these ashes by generating a large volume they end up being dumped carelessly, causing ecological problems [3].

In order to reuse the material of the civil industry and reduce the solid waste, blocks attached to natural fibers can be fabricated. By other hand, the use of natural fibbers changes, not only, the mechanical characteristics, but also the thermal characteristics of the blocks.

In the sector of materials, the infrared thermography (IRT) has found a number each bigger time of uses, especially masonry structures diagnoses. It is justifiable, therefore, when submitted the adverse conditions for which they had been projected, these structures present variations in the integrity standards and, consequently, in the field of temperature. These alterations as presence of humidity, infiltrations, losses of heat and non-apparent inclusions, easily are caught for technique application. The same effect has the change of thermal characteristics.

However, just a few studies have presented a coherent uncertainty analysis that allows validating the results obtained by technique under this respect. By other side, the development of analytical or mathematical models for describing the temporal evolution of the temperature distribution on the surface of a sample should be the main way to predict and better understand the thermographic results [4].

In this work the infrared thermography is applied to the determinate thermal properties – thermal conductivity, thermal diffusivity, emissivity e specific heat – of blocks made from construction waste and natural fibers. A mathematical model was implemented in order to validate the results obtained experimentally by thermographic technique: changing the thermal properties values in the mathematical model, and observing the convergence criteria, it was possible to determine such variables. Regarding the uncertainty analysis, the methodology indicated in [5] and [6] has been used.

### 2. Experimental procedures

Measurement sessions were carried out in the Laboratory of Chemical Engineering of the Centro Universitário de Belo Horizonte – UNIBH.

To perform the analysis were used three types of blocks: the first sample were made with 15% replacement of cement by rice husk ashes; in the second set of samples, coffee husk was used to replace 10% of cement; in the third, 15% of cement was replaced by coffee husk ashes (Figure 1).

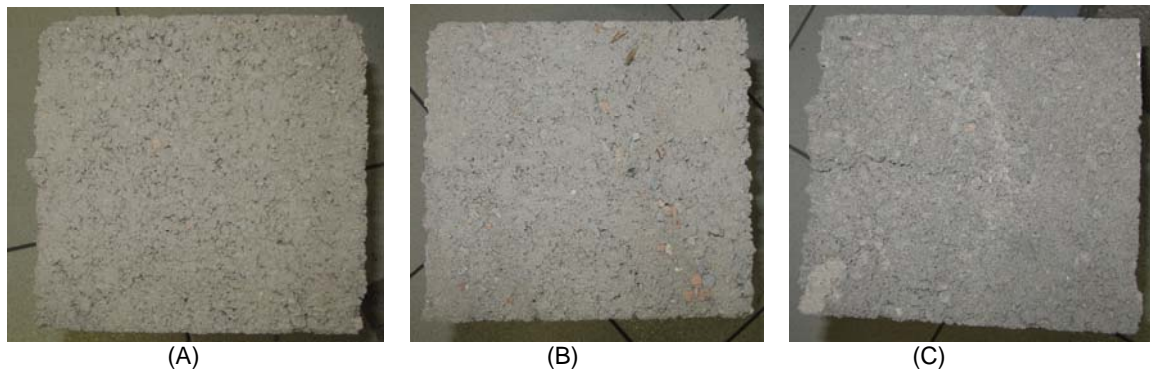


**Fig. 1.** (A) Block made with 15% replacement of cement by rice husk ashes; (B) Block made with 10% replacement of cement by coffee husk ashes; (C) Block made with 15% replacement of cement by coffee husk ashes

Each block has different dimensions and weights, as shown in Table 1.

**Table 1 - Dimensions and weights of the blocks**

Type of Block	15% Coffee	10% Coffee	15% Rice
Length Greater (m)	0,391	0,391	0,391
Width Greater (m)	0,190	0,191	0,191
Height Greater (m)	0,218	0,197	0,206
Length Less (m)	0,160	0,161	0,161
Width Less (m)	0,140	0,141	0,140
Height Less (m)	0,218	0,197	0,206
Weight (Kg)	10,14	9,15	8,98

In determining of the specific mass of the sample was used a scale QUIMIS® model BG 2000. The dimensions of the block were determinate using a digital universal caliper DIGIMESS®. The average of 12 indications for each parameter was obtained and used to determine the specific mass.

The configuration of the thermal bench allows the choice of the distance between the sample and the source of heating (composed of four lamps, each one with power equal to 1000W) and between the thermal camera and the sample. The thermal bench can be seen in Figure 2.



**Fig. 2.** Thermal bench

A detail of the thermal excitation system can be seen in Figure 3.



**Fig. 3.** Thermal excitation system

The thermal camera used in this study was a FLIR I60, whose specifications are presented in Table 2.

**Table 2 – Characteristics of the FLIR I60 thermal camera**

ITEM	SPECIFICATION
Image frequency	9 Hz
Focal distance	0.1 m to infinite
Spatial resolution	2.4 mrad
IR resolution	180 x 180 pixels
Viewing field	25° x 25°
Detector Cooling System	Uncooled microbolometer
Spectral response	7.5 to 13 μm
Thermal sensitivity	< 0.1°C
Observable temperature range (based on black-body temperature)	-20 to +120°C 0 to 350°C
Measurement Uncertainty	± 2°C or ±2% of reading

During the thermal experiments, the testing procedure suggested in [6] has been followed. This methodology considers all the diverse variables involved in the measurement process which gives origin to the measurement uncertainty.

Pulsed thermography was employed. The thermal excitement time used was equal to 10 seconds which allowed the uniform heating of the sample surface. The acquisition time was equal to 90s. The distance between the sample and the thermal camera has been kept to 1.0 m and the distance between the sample and the thermal font at 0.35 m. The environment temperature, indispensable component for the calculation of the measurement uncertainty, was measured using a thermometer with uncertainty equal to ± 0.4°C. The atmospheric transmissivity was considered equal 0.99± 0.01. The emissivity of the surface was determined during the adjustment of the thermal camera. This procedure consist in adjust the emissivity in the thermal camera to indicate the same temperature obtained through contact technique of lesser uncertainty. In this case, thermocouples were installed on the sample surface. The expanded uncertainty of the set thermocouple/temperature indicator was determined to be ± 0.2°C. Image analysis has been conducted using the ThermaCAM Researcher 2002.

In order to ensure the repeatability of the measurement procedure, the tests were repeated 12 times, under identical testing conditions. This procedure allows data uncertainty analysis. Equation 1 has been used to estimate the combined standard uncertainty of the temperature,  $u_c(T_{out})$ , measured by the thermal camera:

$$u_c(T_{out}) = \sqrt{(c_\varepsilon u(\varepsilon_r))^2 + (c_T u(T_{ba(r)}))^2 + (c_\tau u(\tau_{a(r)}))^2 + u_{in}^2} \quad (1)$$

where  $u(\varepsilon_r)$  is the standard uncertainty of determination of the object effective emissivity,  $u(T_{ba(r)})$  is the standard uncertainty of determination of the effective background temperature,  $u(\tau_{a(r)})$  is the standard uncertainty of determination of the effective atmospheric transmittance and  $c_\varepsilon, c_T, c_\tau$  are the sensitivity coefficients equal to partial derivatives of the function  $T_{out}(\varepsilon, T_{ba}, \tau_a)$ . These partial derivatives describe how the output quantity  $T_{out}$  varies with changes in the value of the input quantities  $\varepsilon, T_{ba}, \tau_a$  and can be calculated as:

$$c_\varepsilon = - \frac{\int_0^\infty \frac{\text{sys}(\lambda)}{\lambda^5 [\exp(c_2/\lambda T_{out}) - 1]} d\lambda - \int_0^\infty \frac{\text{sys}(\lambda)}{\lambda^5 [\exp(c_2/\lambda T_{ba(a)}) - 1]} d\lambda}{\int_0^\infty \frac{\varepsilon_a \text{sys}(\lambda) c_2 \exp(c_2/\lambda T_{out})}{\lambda^6 T_{out}^2 [\exp(c_2/\lambda T_{out}) - 1]^2} d\lambda} \quad (2)$$

$$c_T = - \frac{\int_0^\infty \frac{\exp(c_2/\lambda T_{ba(a)}) (1 - \varepsilon_a) \text{sys}(\lambda)}{\lambda^6 T_{ba(a)}^2 [\exp(c_2/\lambda T_{ba(a)}) - 1]} d\lambda}{\int_0^\infty \frac{\varepsilon_a \text{sys}(\lambda) \exp(c_2/\lambda T_{out})}{\lambda^6 T_{out}^2 [\exp(c_2/\lambda T_{out}) - 1]^2} d\lambda} \quad (3)$$

$$c_\tau = - \frac{\int_0^\infty \frac{\varepsilon_a \text{sys}(\lambda)}{\lambda^5 [\exp(c_2/\lambda T_{out}) - 1]} d\lambda - \int_0^\infty \frac{(1 - \varepsilon_a) \text{sys}(\lambda)}{\lambda^5 [\exp(c_2/\lambda T_{ba(a)}) - 1]} d\lambda}{\int_0^\infty \frac{\varepsilon_a \tau_{a(a)} \text{sys}(\lambda) c_2 \exp(c_2/\lambda T_{out})}{\lambda^6 T_{out}^2 [\exp(c_2/\lambda T_{out}) - 1]^2} d\lambda} \quad (4)$$

where  $T_{(ba)a}$  is the ambient temperature during the analysis,  $\varepsilon_a$  is the surface emissivity determined during the tests,  $\tau_{a(a)}$  is the environmental transmissivity during the experiment [6].

To the determination of combined standard uncertainty through Equation 1 is necessary not only to know the coefficients  $c_\varepsilon, c_T$  and  $c_\tau$ , but also the standard uncertainty  $u(\varepsilon_r)$ ,  $(T_{ba(r)})$  e  $u(\tau_{a(r)})$ . Assuming uniform distribution to these variables:

$$u(\varepsilon_r) = \frac{\Delta\varepsilon}{\sqrt{3}} \quad (5)$$

$$u(T_{ba(r)}) = \frac{\Delta T_{ba}}{\sqrt{3}} \quad (6)$$

$$u(\tau_{ba(r)}) = \frac{\Delta\tau}{\sqrt{3}} \quad (7)$$

where  $\Delta\varepsilon, \Delta T_{ba}$  e  $\Delta\tau$  are the standard deviation of the mean for each variable.

In [6] and [7] the authors suggest that, in calculating the combined standard uncertainty it be considered a normal distribution of probabilities once it is applied the central limit theorem. Consequently, the object temperature is definite in the interval  $[T_{out} - u_c(T_{out}) \leq T_{ob} \leq T_{out} + u_c(T_{out})]$ , within which is considered true for a confidence level of 68%. The expanded uncertainty can then be calculated for a confidence level of 95%.

### 3. Mathematical model

The Fourier equation has been used for the mathematical model employed for the numerical simulation of the thermographic investigations, considering a transient state, without heat generation, in three-dimensional Cartesian coordinates. The initial conditions are as follows:

$$T(x, y, z, t) = \frac{Q}{\rho C_p \zeta} \quad \text{for } 0 < z < \zeta \text{ and } t = 0 \quad (8)$$

$$T(x, y, z, t) = T_0 \quad \text{for } z > \zeta \text{ and } t = 0 \quad (9)$$

where  $T$  is the temperature at coordinates  $x, y, z$ , and time,  $t$ ;  $\rho$  is the specific mass of the material;  $C_p$  is the specific heat of the material,  $\zeta$  is the thickness of the last layer of material which covers the surface and absorbs the thermal pulse, and  $T_0$  is the initial temperature of the samples, before thermal excitation.

Because the lateral edges of the sample were isolated during the tests, it was possible to consider a one-dimensional heat flow, in the  $z$  direction, and boundary convection conditions for  $z=0$  and  $z=L$  ( $L$  is the total thickness of the sample). For the convection coefficient, the value  $12 \text{ W}/(\text{m}^2 \cdot ^\circ\text{C})$  was used, which is, approximately, the average of the values adopted for free gas convection [8]. The ambient temperature used in the numerical simulation, was the average of those obtained during the experimental procedures.

In solving the Fourier equation, the finite-volume numerical technique was used. The solution obtained through this technique provides perfect heat balance for the entire calculation domain. A FORTRAN® program has been developed for solving the problem. The number of finite control volumes was defined from grid test and convergence criterion, based on the comparison of the temperature obtained at each point, by the numerical technique, to the temperature obtained analytically (only differences of less than  $10^{-5}$  were accepted) where the domain was considered to be a semi-finite solid. Changing the thermal properties values in the mathematical model, and observing the convergence criteria, it was possible to determine such variables (thermal conductivity, thermal diffusivity and specific heat).

### 4. Results

Figure 4 shows some images during the temperature decay for each sample.

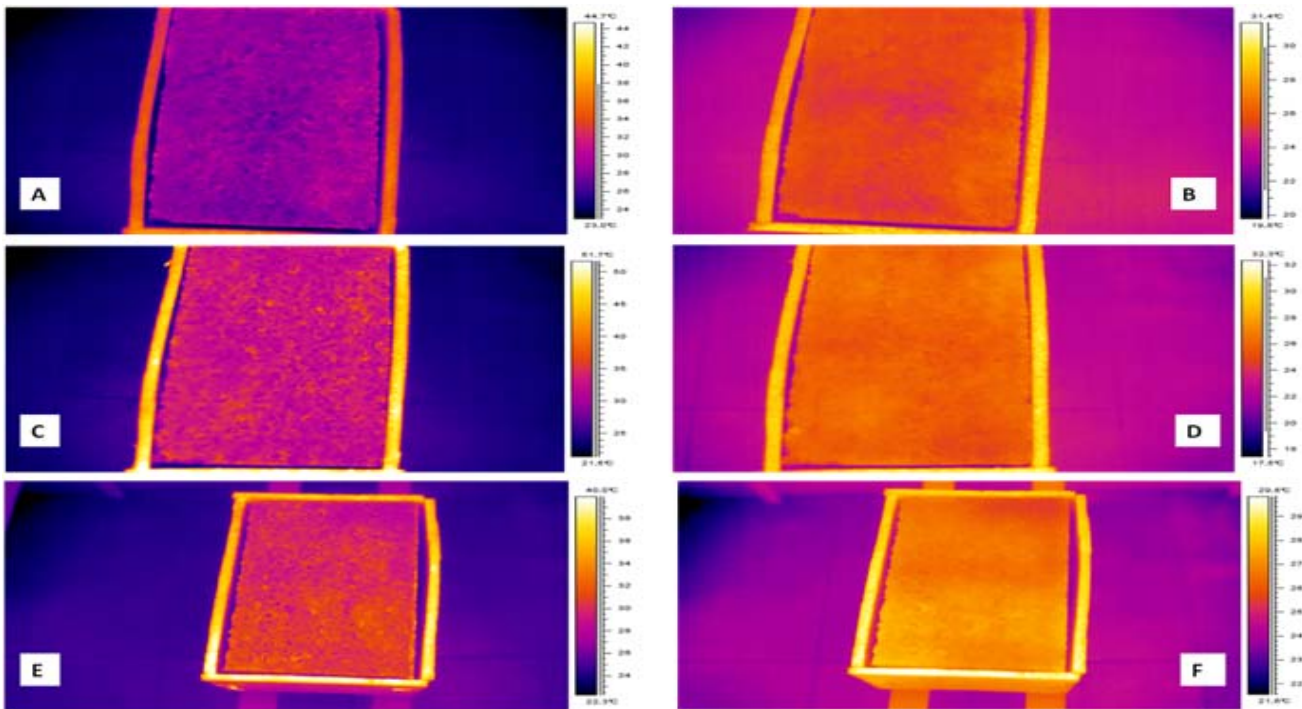


**Fig. 4** – A) Sample 1 at  $t = 0$  s. B) Sample 1 at  $t = 80$  s. C) Sample 2 at  $t = 0$  s. D) Sample 2 at  $t = 80$  s. E) Sample 3 at  $t = 0$  s. F) Sample 3 at  $t = 80$  s.

The images analysis, associated to the mathematical model, allowed the correct identification of the thermal properties of the materials. However, the real characterization of these characteristics is only possible comparing the values obtained for the temperature in the mathematical and experimental models. Figure 5 to 7 presents, for each sample, the superficial temperature decay obtained numerically and experimentally. The maximum uncertainty of measurement, expanded to 95% and calculated according to (1), was  $\pm 1.1^{\circ}\text{C}$ .

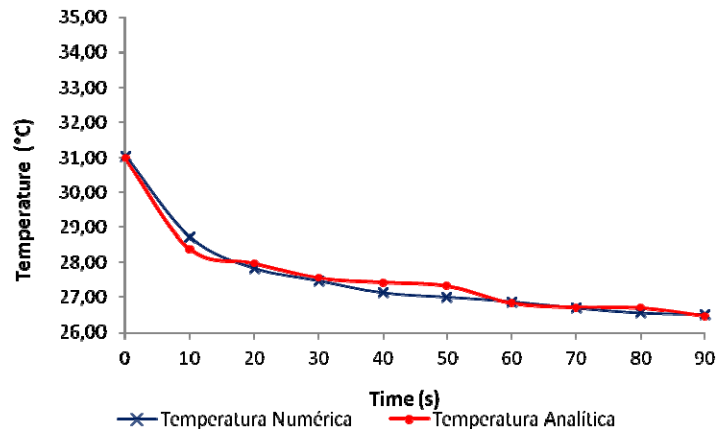


Fig. 5 – Temperature decay of sample 1 – 15% rice husk ashes

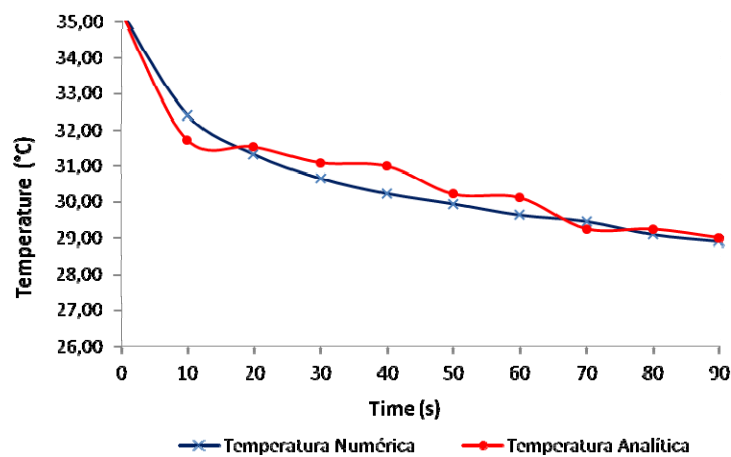


Fig. 6 – Temperature decay of sample 2 – 10% coffee husk ashes

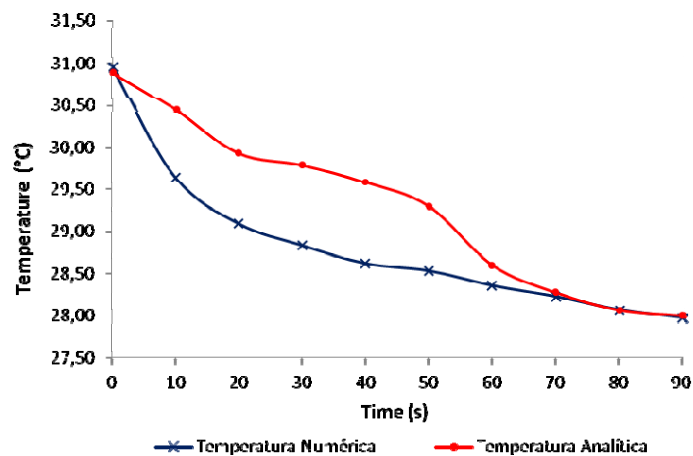


Fig. 7 – Temperature decay of sample 3 – 15% coffee husk ashes

By comparing the theoretical and experimental results, for the transient considered in the analysis, it can be noticed that the difference in temperature between them, for the all the samples, was lower than the uncertainty of measurement, which, in principle, validates the proposed model and, in consequence, the values of variables used.

Although existing, the emissivity problem was controlled during the whole measurement process as well as during image treatment. This permits to calculate the uncertainty component due to this variable.

The procedure permitted to identify the thermal properties of the blocks as showed in Table 3.

**Table 3 – Values of thermal properties**

	<b>Thermal Conductivity</b> [W/(m <sup>2</sup> .K)]	<b>Thermal diffusivity</b> [m <sup>2</sup> /s]
Sample 1	1.22	9.58 x 10 <sup>-7</sup>
Sample 2	1.06	7.26 x 10 <sup>-7</sup>
Sample 3	0.86	5.41 x 10 <sup>-7</sup>

## 5. Conclusions

The aim of this work has been to present the thermography as a tool to identify thermal properties of materials. With this goal experimental testing and mathematical models were implemented.

To perform the analysis were used three types of blocks, manufactured, basically, with waste generated by civil industry where part of the cement was replaced by rice husk ashes and coffee husk ashes. Such waste of the food industry is generated in large volume and end up being dumped carelessly, causing environmental problems.

The experimental results to the superficial temperature were compared with the ones obtained by the mathematical model. In this sense, the thermal properties values have been changed in the mathematical model. It can be noticed that the difference in temperature between the values obtained numerically and experimentally, for the all the samples, was lower than the uncertainty of measurement, which, in principle, validates the proposed model and, in consequence, the values of variables used.

Improvements must be made in the manufacturing process of the blocks in order to improve the uniformity of material and, in consequence, the results. The next stage of work will evaluate the mechanical properties of the blocks, testing new compounds and local fibers. The final goal is to use these blocks in the construction of low income in the state of Minas Gerais.

## 6. Acknowledge

To the Prefeitura de Belo Horizonte and the Ecobloco by their support during the manufacturing of the blocks.

## REFERENCES

- [1] Batista, B.B., Silva, H.R.T., Santos, M.V., Ortiz, P.E., Marcondes, F.L.T. "Bloco verde – reaproveitamento de resíduos da construção civil e de conchas de ostras e mariscos", Santa Catarina, 2009.
- [2] Fioriti, C.F. "Avaliação de compósitos de concreto com resíduos de borracha na produção de blocos para alvenaria". 2002, 134 p. Dissertação (Mestrado em Engenharia Civil) – Faculdade de Engenharia de Ilha Solteira, Universidade Estadual Paulista, São Paulo, 2002.
- [3] Tiboni, R., "A utilização da cinza da casca de arroz de termoeétrica como componente do aglomerante de compósitos à base de cimento Portland", 196 p. Dissertação (Mestrado em Engenharia Civil). Universidade do Estado de São Paulo, São Carlos, 2007.
- [4] Tavares, S. G., Silva, A. M. C., Andrade, R. M. "Theoretical and experimental study of heat diffusion in structures whit internal flaw. In: 18th International Congress of Mechanical Engineering (2005).
- [5] Chrzanowski, K., Fischer, J., Matyszkiew, R., "Testing and evaluation of thermal cameras for absolute temperature measurement", 2000, Journal of Optical Engineering vol. 39, no 9, pp. 2535-254.
- [6] Tavares, S. G. "Desenvolvimento de uma metodologia para aplicação de ensaios térmicos não destrutivos na avaliação da integridade de obras de artes". 169 f. Tese (Doutorado em Engenharia Mecânica) – Departamento de Engenharia Mecânica, Universidade Federal de Minas Gerais, Belo Horizonte, 2006.
- [7] Chrzanowski, K., "Evaluation of thermal cameras in quality systems according to ISO 9000 or EN45000 Standards", Proceedings of SPIE, vol. 4360, pp. 387-401, 2001.
- [8] Incropera, F. P., DeWitt, D. P.. "Fundamentals of heat and mass transfer". Fifth edition, John Wiley & Sons, Inc., New York, (2003).